

Effect of Hydrogen on Evolution of Deformation Microstructure in 2Mn-0.1C Ferritic Steel

1. Introduction

Deterioration of the mechanical properties of metals and alloys by hydrogen is known as hydrogen embrittlement. Hydrogen-related quasi-cleavage (QC) fracture, one of the typical fracture modes of hydrogen embrittlement, occurs along a non-cleavage plane in a transgranular manner. We previously found that the QC fracture propagated parallel to $\{011\}$ planes both in martensitic steel and ferritic steel [1, 2]. These results suggested that the mechanism of the QC fracture is closely related to plastic deformation because $\{011\}$ plane corresponds to the slip plane in body-centered cubic (BCC) crystals. Therefore, further study on the effect of hydrogen on plastic deformation is needed to understand the mechanism of the QC fracture.

In this study, we characterized the evolution of the deformation microstructure in a hydrogen-charged steel with ferrite microstructure [3].

2. Experimental

A 2Mn-0.1C (mass%) steel with ferrite (87%) and pearlite (13%) phases was used in this study. Sheet-type tensile test specimens with a gauge length of 10 mm, a width of 5 mm, and a thickness of 1 mm were cathodically pre-charged with hydrogen in an aqueous solution (3% NaCl + 3 g L⁻¹ NH₄SCN) at a current density of 5 A m⁻². Uniaxial tensile tests were performed at a strain rate of 8.3×10^{-6} s⁻¹, at ambient temperature under hydrogen concurrent-charging condition (same as the pre-charging condition). Some of the tensile tests were stopped and the specimens were unloaded at strain amounts of 3%, 11.5%, 20%, and 24% corresponding to

the end of the Lüders deformation, the middle point of work hardening, the ultimate tensile strength, and prior to the final rupture, respectively.

The tensile-tested and unloaded specimens at strain amounts of 3%–20% were analyzed by neutron diffraction using BL19 “TAKUMI” in J-PARC. From the obtained neutron diffraction profiles, the dislocation densities and the fractions of screw/edge dislocations were evaluated by a convolutional multiple whole profile (CMWP) fitting proposed by Ungar [4]. The microstructures of the tensile-tested and neutron-diffraction-measured specimens were characterized by scanning transmission electron microscopy (STEM). TEM is very useful in characterizing the dislocation morphology, character, and density. However, the disadvantage of TEM is the limited observation area. In contrast, we can obtain bulk average information from neutron diffraction. Using TEM and neutron diffraction together, we characterized the deformation microstructure from bulk to nanoscale.

3. Results and discussion

Figure 1(a) shows the nominal stress–nominal strain curves and dislocation densities. Although the total elongation of the hydrogen-charged specimen (red, 27%) is much smaller than that of the uncharged specimen (black, 48%), the dislocation densities are hardly affected by the presence of hydrogen at the corresponding strain amounts. We note that a certain amount of dislocation that forms cell boundaries is excluded in Fig. 1 because their elastic strain fields mutually cancel each other. Figure 1(b) shows the fractions of screw/edge dislocations estimated from the neutron diffraction

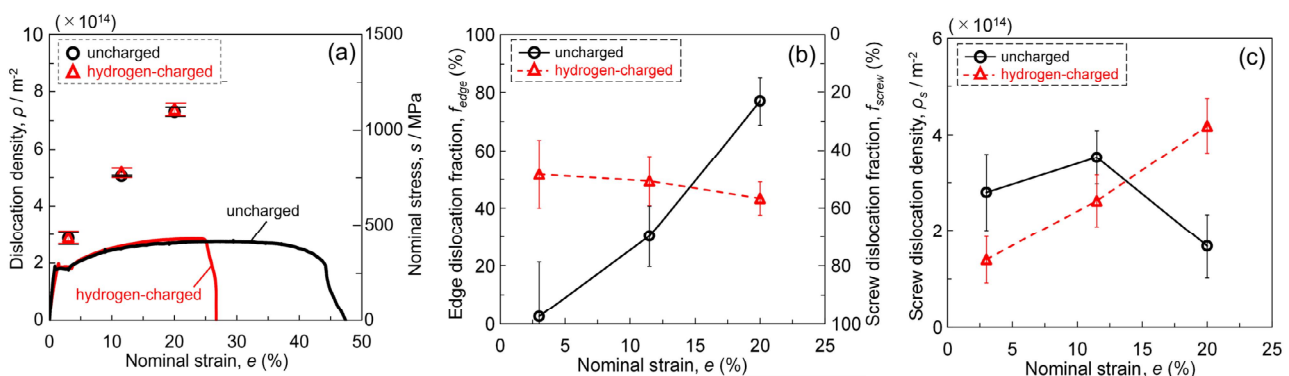


Figure 1. (a) Nominal stress–nominal strain curves and dislocation densities, (b) fractions of screw and edge dislocations, (c) screw dislocation densities of the uncharged specimens (black, circle marks) and the hydrogen-charged specimens (red, triangle marks) [3].

analysis. The left and right axes indicate the fractions of the edge and screw components, respectively. In the uncharged specimens (black circle marks), almost all of the dislocations were screw-type at the initial stage of deformation ($e = 3\%$), and the fraction of the edge component increased monotonically with increasing strain. In contrast, in the hydrogen-charged specimens (red triangle marks), almost equal fractions of screw/edge components were present and did not vary greatly with the strain amount. From the dislocation density data (Fig. 1(a)) and the fractions of the dislocations (Fig. 1(b)), we calculated the individual densities of each type of dislocations. Figure 1(c) shows the changes in the screw dislocation density with strain amount. We found that the screw dislocation density in the hydrogen-charged specimen was much higher than that of the uncharged specimen at the later stage of deformation ($e = 20\%$).

Figures 2(a, d) show low-magnification STEM images of the dislocation morphologies in the uncharged and hydrogen-charged specimens, respectively, at $e = 3\%$. The dislocations are linear in the uncharged specimen, while they are curved and tangled in the hydrogen-charged specimen. To further investigate the deformation microstructure, the nature of the dislocations was characterized. Figures 2(b, e) show high-magnification STEM images of the deformed microstructure in the uncharged and hydrogen-charged specimens, respectively, at $e = 3\%$. Figures 2(c, f) are the schematic illustrations of the dislocation configurations in (b, e),

respectively, where the Burgers vectors of the dislocations determined by the $\mathbf{g} \cdot \mathbf{b} = 0$ invisibility criterion are represented by different colors. In the uncharged specimen, almost all the observed dislocation loops elongated parallel to their Burgers vectors, suggesting that they have a large screw component. On the other hand, in the hydrogen-charged specimen, many dislocations have a large edge component as indicated by arrows in Fig. 2(f). Accordingly, the results demonstrated that the fractions of screw/edge dislocations estimated from the neutron diffraction analysis (Fig. 1(b)) were consistent with the real dislocation nature observed by STEM. We also confirmed that the fraction of each dislocation component was consistent between neutron diffraction and STEM at $e = 20\%$.

It is widely accepted that in BCC transition metals, edge dislocations have greater mobility than screw dislocations because of the higher Peierls potential of screw dislocations, leading to screw-segment-elongated dislocation loops at the initial stage of deformation [5]. This is consistent with the present microstructure in the uncharged specimen. On the other hand, in the hydrogen-charged specimen, many edge-segment-elongated dislocation loops were observed. Thus, the results strongly suggest that the relative velocity of screw dislocation to edge dislocation was increased by hydrogen. Itakura et al. [6] performed first-principles calculations and reported that hydrogen reduced the activation energy for kink-pair nucleation, which led to a

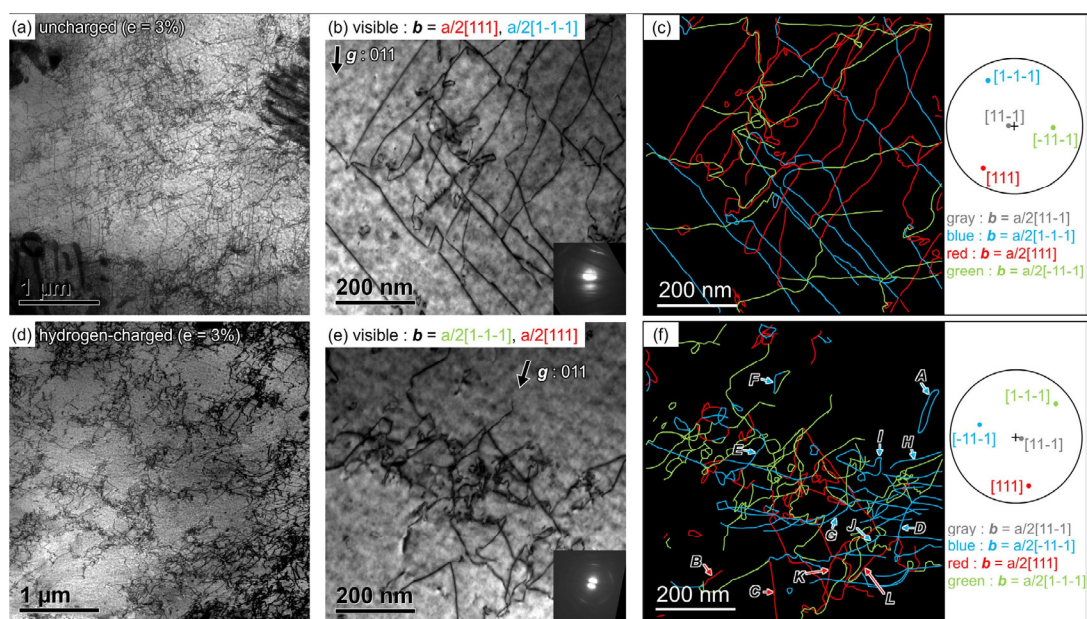


Figure 2. (a, d) low-magnification and (b, e) high-magnification STEM images of the dislocation morphologies under two-beam conditions ($\mathbf{g} = 011$) at a strain amount of 3%. (c, f) Schematic illustrations of the dislocation configurations corresponding (b, e), respectively, where the Burgers vectors of the dislocations determined by contrast analysis are represented by different colors [3]. (a–c) and (d–f) show the uncharged and hydrogen-charged specimens, respectively.

decrease in the critical shear stress for screw dislocation motion. In addition, using molecular dynamics simulations, Matsumoto et al. [7] reported that the motion of edge dislocations was significantly damped by hydrogen. Therefore, we can consider that the tangled dislocation morphology in the hydrogen-charged specimen resulted from the frequent cutting of screw dislocations due to the increase in their relative velocity.

At a strain amount of 24%, well-developed dislocation cell structures, the so-called low energy dislocation structures (LEDS), were observed both in the uncharged and hydrogen-charged specimens. The statistical distributions of LEDS size (d_{LEDS}) and misorientation of LEDS boundaries (θ_{LEDS}) are summarized in Fig. 3(a, b), respectively. The d_{LEDS} was smaller and θ_{LEDS} was larger in the hydrogen-charged specimen than those in the uncharged specimen, suggesting that the amount of dislocation constituting LEDS boundaries was larger in the hydrogen-charged specimen. As explained previously, a certain amount of dislocation constituting the LEDS boundaries was not involved in the dislocation densities derived from the neutron diffraction analysis (Fig. 1(a)). Therefore, the amount of excluded dislocation in the neutron diffraction analysis should be larger in the hydrogen-charged specimen and the density of total dislocations (existing outside the LEDS boundaries and constituting LEDS boundaries) was higher in the hydrogen-charged specimen.

4. Conclusions

In this study, the effect of hydrogen on the evolution of the deformation microstructure in 2Mn-0.1C steel mainly composed of ferrite microstructure was systematically investigated. We found that the densities of the total dislocations (existing outside the LEDS boundaries and constituting LEDS boundaries) were higher in the hydrogen-charged specimens. In addition, we conclude that hydrogen increases the relative mobility of screw dislocations to edge dislocation, leading to the frequent cutting of screw dislocations and tangled dislocation morphology.

5. Acknowledgements

This study was financially supported by JSPS KAKENHI (JP19J21267, JP15H04158, JP19H02459, and JP20K21083) and the Elements Strategy Initiative for Structural Materials (ESISM). The neutron diffraction experiment at the J-PARC was performed under a user program (Proposal No. 2018A0051).

References

- [1] A. Shibata et al., *Mater. Sci. and Technol.*, **33** 1524 (2017).
- [2] K. Okada et al., *Int. J. Hydro. Ener.*, **43** 11298 (2018).
- [3] K. Okada et al., *Acta Mater.*, **225** 117549 (2022).
- [4] T. Ungar et al., *J Appl. Cryst.*, **32** 992 (1999).
- [5] D. Caillard, *Acta Mater.*, **58** 3439 (2010).
- [6] M. Itakura et al., *Acta Mater.*, **61** 6857 (2013).
- [7] R. Matsumoto et al, *Int. ISIJ*, **62** 2402 (2022).

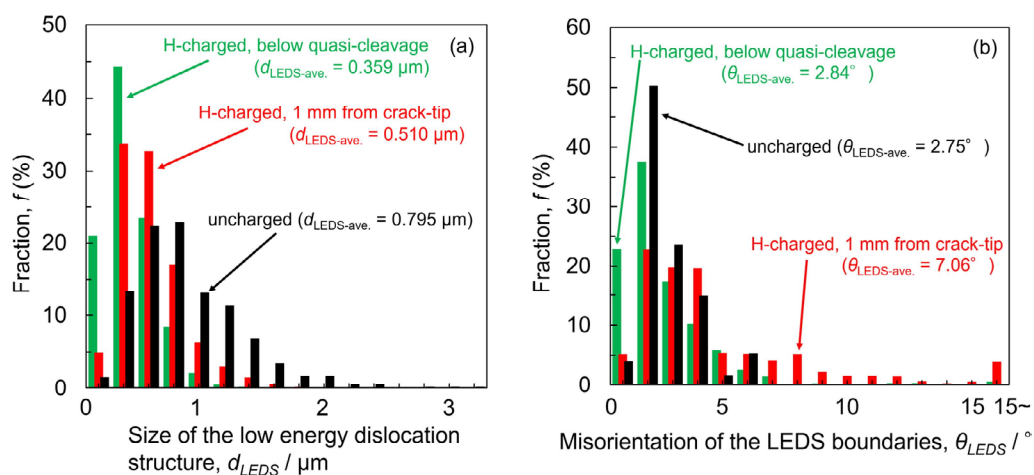


Figure 3. Statistical distribution of (a) LEDS size (d_{LEDS}) and (b) misorientation of LEDS boundaries (θ_{LEDS}) of the microstructures at a strain amount of 24% [3]. The red, green, and black bars indicate areas 1 mm from the crack tip in the hydrogen-charged specimen, just beneath the quasi-cleavage surface in the hydrogen-charged specimen, and the uncharged specimen, respectively.

K. Okada^{1,2}, A. Shibata^{1,3}, W. Gong^{3,4}, and N. Tsuji^{2,3}

¹Research Center for Structural Materials, NIMS; ²Department of Materials Science and Engineering, Kyoto University; ³Elements Strategy Initiative for Structural Materials (ESISM), Kyoto University; ⁴Neutron Science Section, Materials and Life Science Division, J-PARC Center